Mitochondrial Localization and Function of Heme Oxygenase-1 in Cigarette Smoke–Induced Cell Death

Dirk-Jan Slebos*, Stefan W. Ryter*, Marco van der Toorn, Fang Liu, Fengli Guo, Catherine J. Baty, Jenny M. Karlsson, Simon C. Watkins, Hong Pyo Kim, Xue Wang, Janet S. Lee, Dirkje S. Postma, Henk F. Kauffman, and Augustine M. K. Choi

Departments of Pulmonary Diseases and Allergology, University Medical Center Groningen, Groningen, The Netherlands; and Division of Pulmonary, Allergy, and Critical Care Medicine, Department of Medicine, and Center for Biologic Imaging, Department of Cell Biology and Physiology, School of Medicine, University of Pittsburgh, Pittsburgh, Pennsylvania

Cigarette smoke–induced apoptosis and necrosis contribute to the pathogenesis of chronic obstructive pulmonary disease. The induction of heme oxygenase-1 provides cytoprotection against oxidative stress, and may protect in smoking-related disease. Since mitochondria regulate cellular death, we examined the functional expression and mitochondrial localization of heme oxygenase-1 in pulmonary epithelial cells exposed to cigarette smoke extract (CSE), and its role in modulating cell death. Heme oxygenase-1 expression increased dramatically in cytosolic and mitochondrial fractions of human alveolar (A549), or bronchial epithelial cells (Beas-2b) exposed to either hemin, lipopolysaccharide, or CSE. Mitochondrial localization of heme oxygenase-1 was also observed in a primary culture of human small airway epithelial cells. Furthermore, heme oxygenase activity increased dramatically in mitochondrial fractions, and in whole cell extracts of Beas-2b after exposure to hemin and CSE. The mitochondrial localization of heme oxygenase-1 in Beas-2b was confirmed using immunogold-electron microscopy and immunofluorescence labeling on confocal laser microscopy. CSE caused loss of cellular ATP and rapid depolarization of mitochondrial membrane potential. Apoptosis occurred in Beas-2b at low concentrations of cigarette smoke extract, whereas necrosis occurred at high concentrations. Overexpression of heme oxygenase-1 inhibited CSE-induced Beas-2b cell death and preserved cellular ATP levels. Finally, heme oxygenase-1 mRNA expression was elevated in the lungs of mice chronically exposed to cigarette smoke. We demonstrate the functional compartmentalization of heme oxygenase-1 in the mitochondria of lung epithelial cells, and its potential role in defense against mitochondria-mediated cell death during CSE exposure.

Keywords: cigarette smoke; COPD; heme oxygenase-1; mitochondria

CLINICAL RELEVANCE

Cigarette smoke–induced lung cell death contributes to the etiology of chronic obstructive lung disease. This article also contributes to the understanding of the significance of stress protein responses to oxidative stress/injury.

Chronic obstructive pulmonary disease (COPD) ranks among the top five leading causes of death worldwide, with mortality rates still increasing (1). Cigarette smoke (CS), a complex mixture of over 4,000 components including reactive oxygen species (ROS), heavy metals, aldehydes, aromatic hydrocarbons and phenolics, represents the main causative factor in the development of COPD (1–5). To date, the exact pathophysiology of COPD remains unknown, thus very few effective treatment modalities exist (5, 6). In susceptible smokers, CS exposure potentially results in chronic inflammation of the airways, leading to airways obstruction and an alveolar wall inflammatory response associated with lung cell death, lung tissue destruction, and emphysema (2, 5, 7).

ROS may directly participate in specific tissue injury and cell death (both apoptosis and necrosis) in COPD (3, 8, 9). A significant portion of cellular ROS arises in mitochondria, associated with the leakage of partially reduced oxygen from the electron transport chain under normal and pathologic conditions. In addition, mitochondria regulate apoptosis induced by extracellular signals through the release of pro-apoptotic mediators (e.g., cytochrome c, apoptosis-inducing factor) (10). Furthermore, mitochondria serve as the principal energy source of the cell through the production of ATP. Cellular ATP levels play an essential role in the determination of apoptotic or necrotic cell fate (11). Many constituents of CS can accumulate in the mitochondria and perturb mitochondrial respiratory chain function, thereby affecting cellular ATP production (12–14).

Heme oxygenase-1 (HO-1; E.C. 1:14:99:3), which catalyses the rate-limiting step in the oxidative degradation of heme (15, 16), confers protection against exogenous stresses and inhibits apoptotic cell death in a variety of disease states (17–19). The mechanisms by which HO-1 provides protection likely involve its enzymatic reaction products: carbon monoxide (CO), biliverdin-IXα, and ferrous iron (17–19). The transcriptional induction of HO-1 responds to a wide variety of cellular stress, including oxidants and altered states of oxygen tension, identifying this response as a major inducible cellular defense mechanism (19). We have recently shown a lower expression of HO-1 in ex-smoking patients with COPD compared with ex-smoking healthy control subjects (20). A $(GT)_n$ dinucleotide length polymorphism that is linked to the development of COPD has been described in the promoter region of HO-1, resulting in a lower expression of HO-1 in people who have the polymorphism (21). Thus, a genetically dependent down-regulation of HO-1 expression may arise in subpopulations, possibly linked to increased susceptibility to the pathologic consequences of ROS (22).

Together, these observations led to the hypothesis that HO-1 exerts a potential regulatory and/or protective function in COPD

(*Received in original form June 14, 2006 and in final form September 29, 2006*)

* Equal contribution as first author.

This study was financially supported in part by the department of internal medicine of the University Medical Center Groningen, The Netherlands to D.-J.S. and by a Dutch Kidney Foundation grant to M.v.d.T. This work was also supported by awards from the American Heart Association to S.W.R. (AHA #0335035N) and H.P.K. (AHA #0525552U), and by NIH grants R01-HL60234, R01-AI42365, and R01-HL55330 to Principal Investigator A.M.K.C.

Correspondence and requests for reprints should be addressed to Augustine M. K. Choi, M.D., Division of Pulmonary, Allergy and Critical Care Medicine, Department of Medicine, MUH 628NW, 3459 Fifth Ave., Pittsburgh, PA 15213. E-mail: Choiam@upmc.edu

Am J Respir Cell Mol Biol Vol 36. pp 409–417, 2007
Originally Published in Press as DOI: 10.1165/rcmb.2006-0214OC on November 1, 2006
Internet address: www.atsjournals.org

by preserving mitochondrial function, and by inhibiting cell death associated with CS exposure. Therefore, we sought to characterize the potential localization of HO-1 in the mitochondria and its function with respect to cell survival.

Given the historical characterization of HO-1 as a resident of the endoplasmic reticulum (ER), we have recently observed the redistribution of HO-1, after stress induction, to various subcellular fractions, including caveolae and cytochrome c–containing fractions (23). This work was the first to suggest the potential localization of HO-1 to the mitochondria and provided the rationale for the current study. We demonstrate the mitochondrial compartmentalization of active HO-1 protein, and its accumulation in this organelle in response to discrete forms of cellular stress. Furthermore, these observations have been made in the context of pulmonary epithelial cells treated with aqueous cigarette smoke extract (CSE) as a specific *in vitro* model of CS exposure. We also demonstrate that HO-1 protects epithelial cells against CSE-induced cell death, in part by preserving cellular ATP production. These studies expand our knowledge of the subcellular distribution and functional significance of HO-1, as it relates to CS-induced cellular injury.

MATERIALS AND METHODS

Materials

All reagents were from Sigma (St. Louis, MO) unless otherwise indicated. Bovine hemin (ferriprotoporphyrin-IX chloride), and tin protoporphyrin-IX (SnPPIX) (Frontier Scientific, Logan, UT) were dissolved in dimethyl sulfoxide as 10 mM stock solutions, and stored at –20°C. The hemin was dissolved in cell culture media to a working concentration of 10 μM. Lipopolysaccharide (LPS) was freshly prepared and used for experiments at a concentration of 100 ng/ml. JC-1 (5,5′,6,6′-tetrachloro-1,1′,3,3′ tetraethylbenzimidazolylcarbocyanine iodide/chloride) was from Invitrogen (Carlsbad, CA).

Preparation of CSE

Kentucky 1R3F research-reference filtered cigarettes (The Tobacco Research Institute, University of Kentucky, Lexington, KY) were smoked using a peristaltic pump (VWR International, West Chester, PA). Before the experiments, the filters were cut from the cigarettes. The smoke was bubbled through cell growth medium. Each cigarette was smoked in 6 min with a 17-mm butt remaining. Four cigarettes were bubbled through 20 ml of medium, and this solution was regarded as 100% strength CSE. The 100% CSE was adjusted to a pH of 7.45 and was used within 15 min after preparation.

Cell Culture

A549 and Beas-2b lung epithelial cells were purchased from American Type Culture Collection (ATCC, Manassas, VA). A549 cells were cultured in Ham's F-12 medium supplemented with 10% FBS and 0.1% gentamycin (Gibco-Invitrogen, Carlsbad, CA) in a humidified atmosphere of 5% CO_2/balanced air at 37°C. Beas-2b cells were cultured according to the ATCC prescription in the serum-free medium BEGM (Cambrex, East Rutherford, NJ). Before the experiments the A549 or Beas-2b cells were cultured for 16 h in serum-free F-12 media or growth factor-free media (BEBM; Cambrex), respectively. Small airway human bronchial epithelial cells were purchased as frozen primary cultures from Clonetics Ltd (Walkersville, MD). They were cultured in the manufacturer's basal medium (SAGM) and supplements.

Western Blot Analysis

The following antibodies were used for immunoblotting: anti-heme oxygenase-1 (1:2,000), anti-NADPH cytochrome p450 reductase (NPR), anti-biliverdin reductase (BVR) (Stressgen, Victoria, BC, Canada), anti–cytochrome c, anti–β-actin (Santa Cruz, Santa Cruz, CA), or anti-p110 (Calbiochem, San Diego, CA). Western immunoblot analyses were performed as previously described (23).

Mitochondrial Isolation

A549 and Beas-2b cells were harvested in 0.05% digitonin in an extraction buffer containing 10 mM Hepes, pH 7.5, 150 mM NaCl, 1 mM EGTA, and 1.5 mM $MgCl_2$. The cell extracts were spun at 700 × *g* for 10 min. The supernatants were transferred to new tubes and centrifuged again at 30,000 × *g* at 4°C for 30 min. The resulting supernatants were removed, and the pellets were either retained for Western blotting, or for assessment of HO-enzyme activity. Alternatively, mitochondria were isolated using a commercial mitochondria isolation kit (Sigma-Aldrich Chemie B.V., Zwijndrecht, The Netherlands) and suspended in respiratory buffer (120 mM KCl, 5 mM K_2PO_4, 3 mM HEPES, 1 mM EGTA, pH 7.2). Mitochondrial protein content was determined by the Bradford method (Bio-Rad Laboratories, Veenendaal, The Netherlands) according to the manufacturer's instructions. Both extraction methods gave comparable results in Western immunoblot analyses.

Heme Oxygenase Activity

Heme oxygenase activity was measured in both whole cell and mitochondrial fractions by the spectrophotometric determination of bilirubin production as previously described (24). HO activity was reported as pmol bilirubin/mg protein/h assuming an extinction coefficient of 40 mM^{-1} cm^{-1} for bilirubin in chloroform.

Immunofluorescence Labeling and Confocal Laser Microscopy

Beas-2b cells were grown on 35 mm/10 mm glass-bottom culture dishes (MatTek Corp., Ashland, MA). After experimental treatments, cells cultured under standard growth conditions at 37°C were stained for mitochondria using the Mitotracker Red dye (M-7513; Molecular Probes, Eugene, OR), at 1 μM for 45 min. Cells were then washed with PBS, fixed, and permeabilized in 2% paraformaldehyde with 0.1% Triton-X100. Cells were then washed with PBS and wash buffer (0.5% bovine serum albumin, 0.15% glycine in PBS), and blocked with 10% goat serum in wash buffer. Immunostaining was performed using a polyclonal HO-1 antibody (1:1,000; Stressgen), and goat anti-rabbit Alexa 488–conjugated secondary antibodies (1:1,000; Jackson ImmunoResearch Laboratories, West Grove, PA). Cells were viewed with an Olympus Fluoview BX 61 confocal microscope (Olympus, Center Valley, PA) and images were collected using a DC-330S cooled CCD camera (DAGE-MTI, Michigan City, IN).

Transition Electron Microscopy

After experimental manipulations, Beas-2b cells were washed with PBS and fixed in 2.5% glutaraldehyde in PBS. The cells were photographed using a JEOL JEM 1210 transmission electron microscope (JEOL, Peabody, MA) at 80 or 60 kV onto electron microscope film (ESTAR thick base; Kodak, Rochester, NY) and printed onto photographic paper. Rabbit anti–HO-1 polyclonal antibody (Stressgen) suitable for IHC was used for gold-immunostaining.

Annexin V–Fluorescein Isothiocyanate Propidium Iodide Staining

Annexin V–fluorescein isothiocyanate (FITC)/propidium iodide (PI) staining was performed using the FITC-labeled annexin V kit (BD Pharmingen, San Diego, CA), according to the manufacturer's protocol. Labeled cells were analyzed using a FACS-Calibur (BD Biosciences, San Jose, CA).

Transfections

Adenovirus–ho-1 (Ad-HO-1) and adenovirus-LacZ (Ad-LacZ) were supplied by the Center for Biotechnology and Bioengineering, University of Pittsburgh, Pittsburgh, PA (www.vectorcore.pitt.edu). Beas-2b cells were grown to subconfluence and starved overnight. Ad-HO-1 and Ad-LacZ were added to culture media at 50 plaque-forming units per cell. After 6 h the medium containing the virus was changed to regular growth medium and the experiment were performed 24 h from the initiation of transfection.

Adenosine Triphosphate Assay

ATP was measured using an ATP-luciferase assay kit (Calbiochem) using the manufacturer's instructions and standards. Beas-2b cells were

seeded at 5×10^3 cells/well in opaque 96-well microplates (BD Falcon, Bedford, MA) and grown under standard cell culture conditions for 48 h before the experiments. Luciferase activity was measured within 1 min of reagent addition using a luminometer (Lmax; Molecular Devices, Sunnyvale, CA).

Determination of Mitochondrial Membrane Potential

JC-1 is a cationic dye that is accumulated into mitochondria in a membrane potential–dependent manner. Upon accumulation within the mitochondria, the dye forms aggregates (J-aggregates) that emit a red fluorescence imaged with standard rhodamine optical filters. In the presence of depolarized mitochondria the dye remains dispersed within the cytoplasm as a monomer, emitting a green fluorescence detected with FITC filters. Therefore, depolarization of mitochondria can be detected as an increase in the green/red fluorescence intensity ratio. The excitation, dichroic, and emission wavelengths are 485 ± 11 nm, 505 nm, and 530 ± 15 nm for the monomer, and 535 ± 17.5 nm, 570 nm, and 590 ± 17.5 nm for the J-aggregate, respectively.

Normal Beas-2b were grown to 50% confluence on Lab-Tek four-well chambered coverglass (Nalge Nunc, Rochester, NY) overnight and then were incubated for 30 min at 37°C in the presence of 1 μg/ml JC-1 (Invitrogen, Carlsbad, CA), and then washed. Cells were maintained at 37°C in a heated microincubator (Harvard Apparatus, Inc., Hamden, CT) in HEPES-buffered media during imaging. Images were acquired at five different positions in a given chamber, using an Olympus IX81 with ×20 objective (0.70 NA) and Retiga EXi CCD camera (Q-Imaging, Burnaby, BC, Canada), every 30 s for a 5 min baseline; then media or CSE was added and imaging was continued for an additional 20 min. Hydrogen peroxide was added to the media at 1 mM for a positive control. MetaMorph 6.3 (Molecular Devices) was used for image acquisition and subsequent analysis. In calculating the green/red fluorescence ratio, background correction was used for each image and time point. Data are reported as the average change in the green/red ratio for each cell over a 20-min exposure interval, normalized to corresponding average baseline. Data represent mean average change for three to five independent positions, in which 20 cells were analyzed for each position.

In Vivo Cigarette Smoke Exposure

Animals were housed according to guidelines from the American Association for Laboratory Animal Care and Research Protocols and were approved by the Animal Care and Use Committee (University of Pittsburgh School of Medicine). Male, age-matched AKR/J strain mice (Jackson Laboratories, Bar Harbor, ME) were exposed to CS or filtered air under identical conditions beginning at 8 wk of age. Total body CS exposure was performed in a stainless steel chamber (71 cm × 61 cm × 61 cm) using a smoking machine (Model TE-10; Teague Enterprises, Woodland, CA), similar to that reported by others (25, 26). The smoking machine puffs each 1R3F cigarette for 2 s, for a total of 9 puffs before ejection, at a flow rate of 1.05 liters/min, providing a standard puff of 35 cm^3. The smoke machine was adjusted to deliver five cigarettes at one time. Mice were exposed 5 d/wk for up to 24 wk. The chamber atmosphere was periodically measured for total particulate matter concentrations of ~ 120 mg/m^3. Carboxyhemoglobin levels in the AKR/J strains of mice after 2 wk of cigarette exposure were < 8% immediately after exposure.

Real-Time PCR

At 2, 12, and 24 wk, control or CS-exposed mice were killed by an overdose of pentobarbital, injected intraperitoneally. The left lung was removed during necropsy, snap-frozen immediately in liquid nitrogen, and stored at −80°C till use. Lung tissue was homogenized and RNA extracted using the TRIZOL method (Invitrogen, Carlsbad, CA). The RNA samples were reverse transcribed into cDNA, which served as template for quantitative RT-PCR. Probes and primers for the HO-1 gene as well as the TaqMan Master Mix containing the necessary reagents for gene expression studies were obtained from Applied Biosystems (Foster City, CA). Gene expression was analyzed by the delta delta Ct method, with 18 s rRNA as the endogenous control. The average dCT of age-matched air-exposed AKR/J male mice served as the calibrator. Three to eight animals in each group were used for each time point measured.

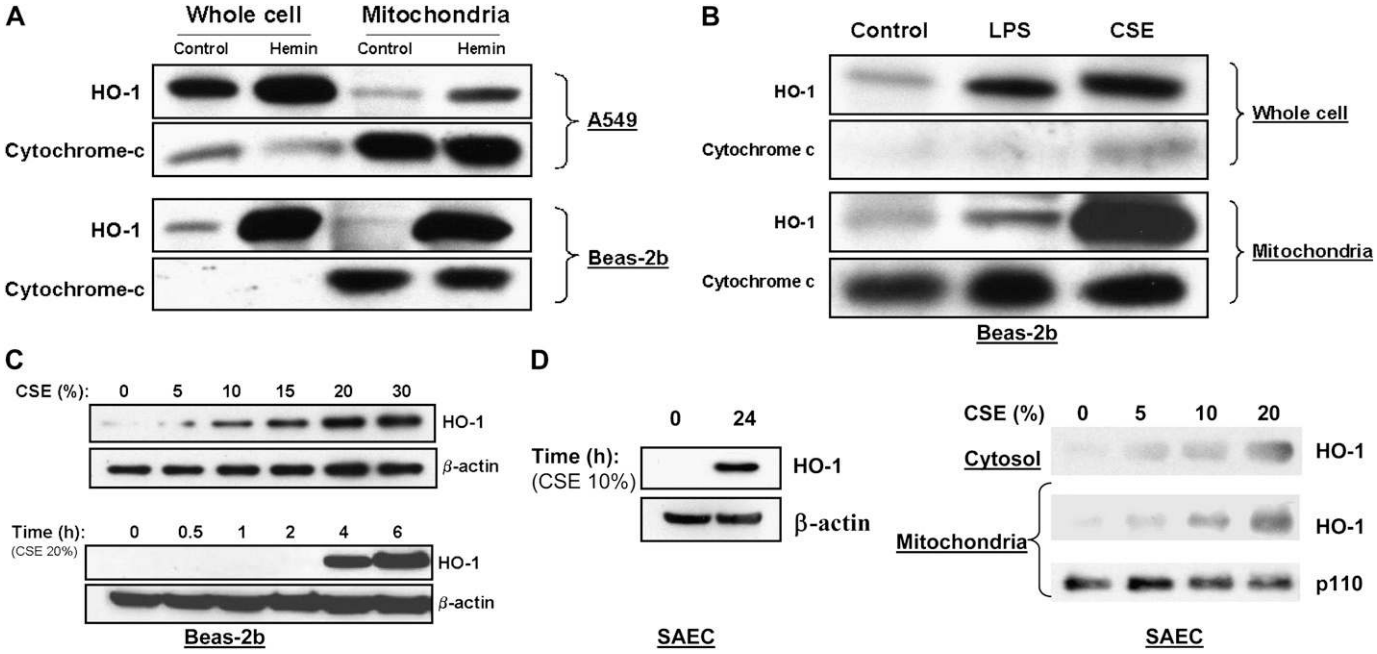

Figure 1. CSE and stress treatments result in mitochondrial accumulation of HO-1 protein in epithelial cells. (*A*) A549 cells or Beas-2b cells were treated in the absence (control) or presence of hemin (10 μM) for 18 h. (*B*) Beas-2b cells were treated with LPS (0.1 μg/ml) or CSE (15%) for 18 h. (*C*) Beas-2b cells were starved overnight in growth factor–free media and then treated with varying concentrations of CSE (0–30%) for 4 h, or with a fixed dose (20%) for 0–6 h. (*D*) Primary small airway epithelial cells (SAEC) were cultured as described in MATERIALS AND METHODS, and treated with varying concentrations of CSE (10% for 0–24 h, *left panel*) or (0–20% for 24 h, *right panel*). Cells were harvested and fractionated into either whole cell or mitochondrial fractions as described in MATERIALS AND METHODS. Samples containing equivalent amounts of protein were subjected to SDS-PAGE and Western immunoblot analysis for expression of HO-1 (*A–D*). Cytochrome-c (*A, B*) or mitochondrial p110 (*D*) served as a marker of the relative content of mitochondrial protein. β-Actin served as a standard for protein loading in whole cell experiments (*C, D*).

Statistical Analysis

All values were expressed as the mean ± S.D. from at least three independent experiments. Differences in measured variables between experimental and control group were assessed using the Student's *t* test (Statview II Statistical Package; Abacus Concepts, Berkeley, CA). Statistically significant difference was accepted at $P < 0.05$. *In vivo* gene expression data were analyzed using the rank-sum Mann Whitney U test for non-normally distributed data.

RESULTS

HO-1 Is Expressed in Mitochondria in Response to Stimuli

To examine the inducible stress response in lung epithelial cells, A549 and Beas-2b cells were treated with hemin (10 μM), a potent inducer and substrate of HO-1, for 18 h. As expected, HO-1 protein expression increased in response to hemin treatment in both cell lines (Figure 1A). Surprisingly, inducible HO-1 expression appeared in the mitochondrial fractions of both cell lines after heme treatment (Figure 1A). To examine whether this phenomenon also occurred in response to other known inducers of the HO-1 response, independently of substrate loading (hemin), Beas-2b cells were exposed to either bacterial LPS (0.1 μg/ml) or CSE (15%) for 18 h. While both stimuli also induced HO-1 protein expression in whole cell and mitochondrial fractions, the CSE treatment produced the most dramatic mitochondrial accumulation of HO-1 (Figure 1B). Furthermore, CSE induced HO-1 in Beas-2b cells in a dose-responsive and time-dependent manner (Figure 1C). In addition to the epithelial cell lines, the response was also observed in human primary small airway epithelial cells (SAEC) (Figure 1D). HO-1 accumulated in whole cells, and in mitochondrial fractions of SAEC in a dose-dependent fashion after 24 h continuous CSE exposure.

Mitochondrial HO-1 Is Highly Inducible and Functionally Active

The functional activity of HO-1 in whole cell and mitochondrial extracts after stress treatments was verified by spectrophotometric determination of bilirubin production. Beas-2b cells were subjected to hemin (10 μM) or CSE (15–20%) for 18-h exposures, followed by the isolation of mitochondrial protein and whole cell lysates. As expected, both hemin and CSE (20%) induced HO activity in whole cell extracts from a basal activity of 175 ± 28 pmol bilirubin/mg protein/h, approximately 4- to 5-fold (hemin: 849 ± 114; CSE: 675 ± 35 pmol bilirubin/mg protein/h) (Figure 2A), which correlated with HO-1 protein expression at this time point. HO activity in the mitochondrial fractions increased from 13-fold (for hemin), up to 19 fold after CSE treatment relative to the basal mitochondrial HO activity (308 ± 58 pmol bilirubin/mg mitochondrial protein/h) (Figure 2B). In addition, we examined the mitochondrial localization of enzymes

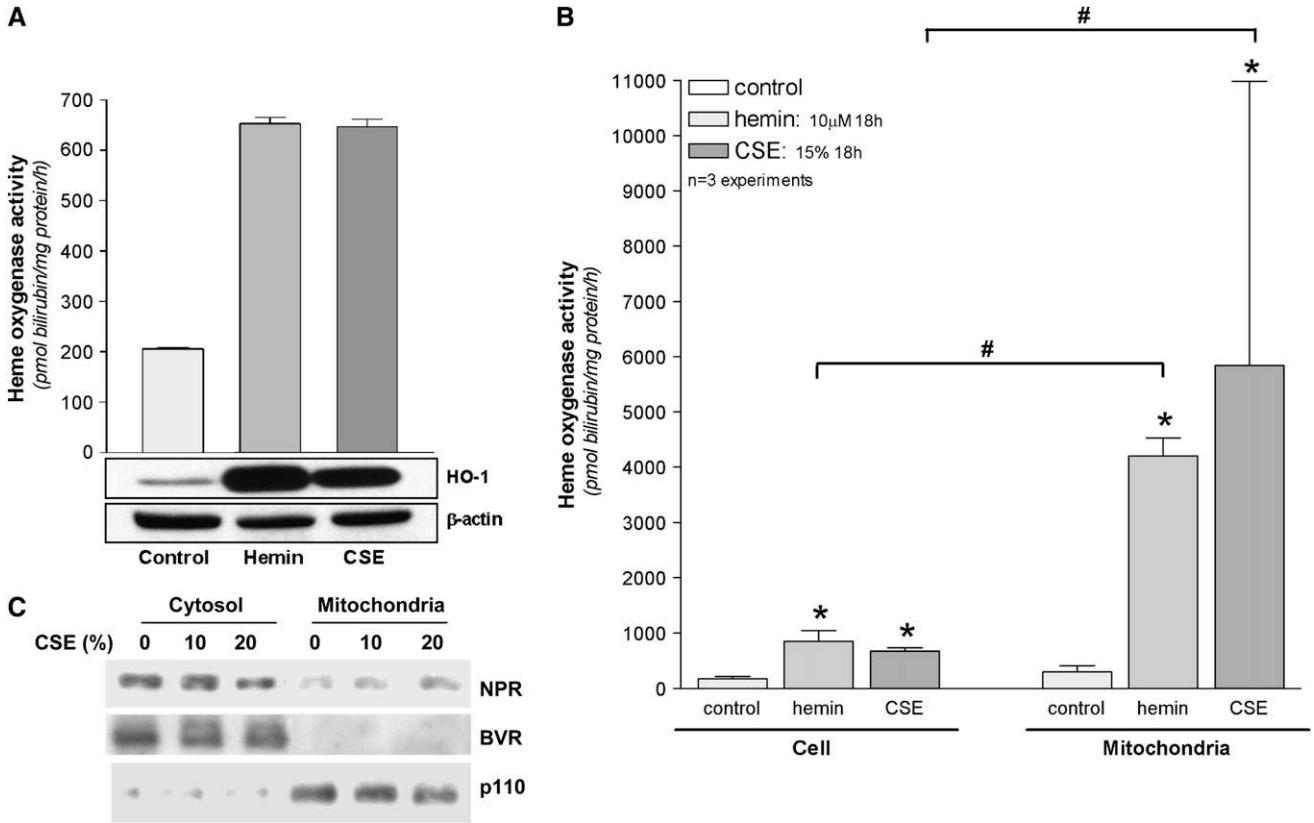

Figure 2. Cellular or mitochondrial HO-1 induced by CSE and heme is functionally active. (*A*) Beas-2b cells were subjected to heme (10 μM) or CSE (20%) for 18 h. Corresponding whole cell extracts were analyzed for HO activity and HO-1 protein by Western immunoblot analysis. β-Actin served as a standard for protein loading. Western blots are representative of three independent experiments. (*B*) Beas-2b were subjected to heme (10 μM) or CSE (15%) for 18 h. Corresponding whole cell and mitochondrial extracts were analyzed for relative HO activity. Activity data represent mean ± SD of three independent experiments ($n = 3$), each with triplicate determinations $^*P < 0.05$, #relative to corresponding whole cell extract. Units represent pmol bilirubin/mg protein (cellular or mitochondrial)/h (*A, B*). (C) Beas-2b treated with CSE (10–20%) or media were harvested and fractionated into either whole cell or mitochondrial fractions as described in Materials and Methods. Samples containing equivalent amounts of protein were subjected to SDS-PAGE and Western immunoblot analysis for expression of NADPH cytochrome p450 reductase (NPR) or NAD(P)H biliverdin reductase (BVR). Mitochondrial p110 served as a marker of the relative content of mitochondrial protein.

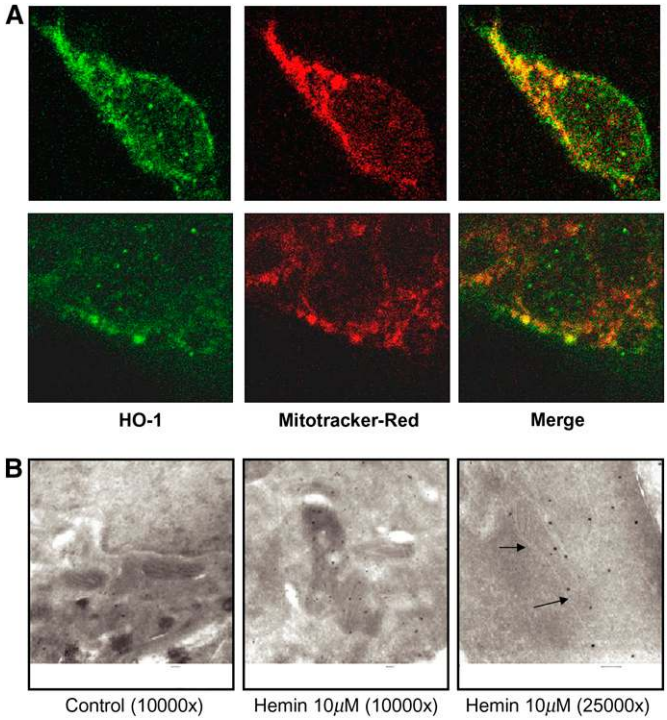

Figure 3. HO-1 co-localizes with mitochondria. Beas-2b cells were starved overnight in growth factor–free media, and then treated with hemin (10 μM) for 18 h. (*A*) Cells were stained with mitotracker Red, and immunostained with HO-1 antibody as described in MATERIALS AND METHODS. *Upper* and *lower panels* are two representative series from different cells. (*B*) Alternatively, cells were immunogold-stained for HO-1 and analyzed with scanning electron microscopy. The *arrows* show the position of the mitochondrial membrane.

associated with HO activity. NADPH cytochrome p-450 reductase was detected in the mitochondrial fractions of Beas-2b cells, but did not vary significantly in response to CSE treatment. NADPH biliverdin reductase (BVR), in contrast, was not detected in the mitochondria of Beas-2b cells (Figure 2C).

Immunofluorescence staining for confocal laser microscopy revealed a colocalization of HO-1 expression and mitochondrial staining in Beas-2b cells after hemin treatment (Figure 3A). We further confirmed the mitochondrial localization of HO-1 using immunogold labeling on electron microscopy (Figure 3B).

CSE Induces Both Apoptosis and Necrosis in Lung Epithelial Cells

To investigate the CSE-induced cell death process in lung epithelial cells, Beas-2b cells were exposed to a high concentration of CSE (50%) for 0–5 h, and apoptosis and necrosis were assessed simultaneously by using the annexin V–FITC/PI assay (Figures 4A and 4B). A peak in the annexin V–FITC signal appeared after 1 h exposure, and decreased in the hours thereafter. The percentage of PI (necrotic cells) however, increased after the first hour, and continued to increase until the last hour measured (5 h). To examine the dose-dependency of the occurrence of apoptosis and necrosis, we exposed the Beas-2b cells to different concentrations of CSE for 3 h. Below a concentration of 30% CSE, almost exclusively annexin V–FITC positive cells (apoptosis) were observed. The percentage of apoptotic cells increased linearly and dose-dependently between CSE concentrations of 0–20%, reaching an apparent maximum at 20% CSE, whereas the appearance of cellular necrosis began at concentrations of CSE at 30% and higher (data not shown). We furthermore observed the time-dependent activation of caspase-3 after exposure of Beas-2b cells to 30% CSE, beginning as early as 30 min after exposure and persisting at least 12 h (data not shown).

At a concentration of 30%, CSE caused rapid mitochondrial membrane depolarization, a hallmark of apoptosis, which exceeded that produced by addition of 1 mM H_2O_2 (Figure 4C).

HO-1 Expression Protects Epithelial Cells from CSE-Induced Cell Death and ATP Depletion

Beas-2b cells were infected with an adenoviral construct containing *ho-1* cDNA (Ad-HO-1) or *LacZ* cDNA (Ad-LacZ). HO-1–overexpressing cells or corresponding Ad-LacZ–infected controls were subjected to challenge with 30% CSE for 3 h, or to an equivalent amount of complete growth media for 3 h. CSE dramatically reduced cellular ATP levels in Ad-LacZ–infected controls, which were further depressed by inclusion of the HO inhibitor tin-protoporphyrin-IX (SnPPIX, 20 μM). In contrast, CSE failed to depress cellular ATP levels in HO-1–expressing cells. Inclusion of SnPPIX reversed the protection conferred by Ad-HO-1, and resulted in depleted ATP levels (Figure 5A). CSE treatment (30%) for 3 h caused necrotic cell death in LacZ-expressing controls. HO-1 expression as a result of Ad-HO-1 infection reduced cellular necrosis relative to LacZ controls, after CSE challenge (30%, 3 h) (Figure 5A). These experiments demonstrate a general protective effect of HO-1 against necrosis and associated depletion of cellular energy charge during exposure to CSE.

Chronic CS Exposure Up-Regulates HO-1 Expression in the Lungs of Mice

We examined the expression of *ho-1* in the lung after chronic exposure to CS *in vivo*. Mice exposed to CS displayed dramatically elevated expression of *ho-1* mRNA after 2 wk of chronic CS exposure relative to air-exposed controls. The elevated *ho-1* mRNA expression persisted up to 12 wk of CS exposure. *ho-1* mRNA expression returned to control values after the 24th week of continuous CS exposure (Figure 6).

DISCUSSION

Injury of the alveolar epithelium by CS constituents plays a role in the pathogenesis of COPD (2). The mechanisms underlying CS-induced epithelial cell death, however, remain unclear. It has been shown that CSE causes dose- and time-dependent cell death in A549 alveolar epithelial cells (27). Furthermore, low concentrations of CSE induce apoptosis, whereas higher concentrations induce necrosis in these cells (27). Similar transition from apoptotic to necrotic phenotype with increasing CSE dose was also observed in a human premonocytic line (U-937) (28). Apoptotic phenotypes appeared in other lung cell types exposed to CSE, including alveolar macrophages (29) and human lung fibroblasts (30), as well as in mainstream CS-treated rat bronchial/bronchiolar epithelial cells (31). Antioxidant compounds (N-acetyl-L-cysteine) alone, or in combination with other scavengers (e.g., aldehyde oxidase) protected against CSE-mediated apoptosis in several models, implying the involvement of CSE-derived and/or intracellular reactive species (27–29). In alveolar macrophages, CSE induced apoptosis by activating an intrinsic mitochondria-dependent pathway, involving increased ROS generation, mitochondrial dysfunction, Bax accumulation, cytochrome-c release, independently of p53, Fas, or caspase activation (28). Similar observations of ROS- and mitochondria-dependent apoptosis were observed after CSE exposure in various nonpulmonary cell types (28, 32–34). In human gastric adenocarcinomas and

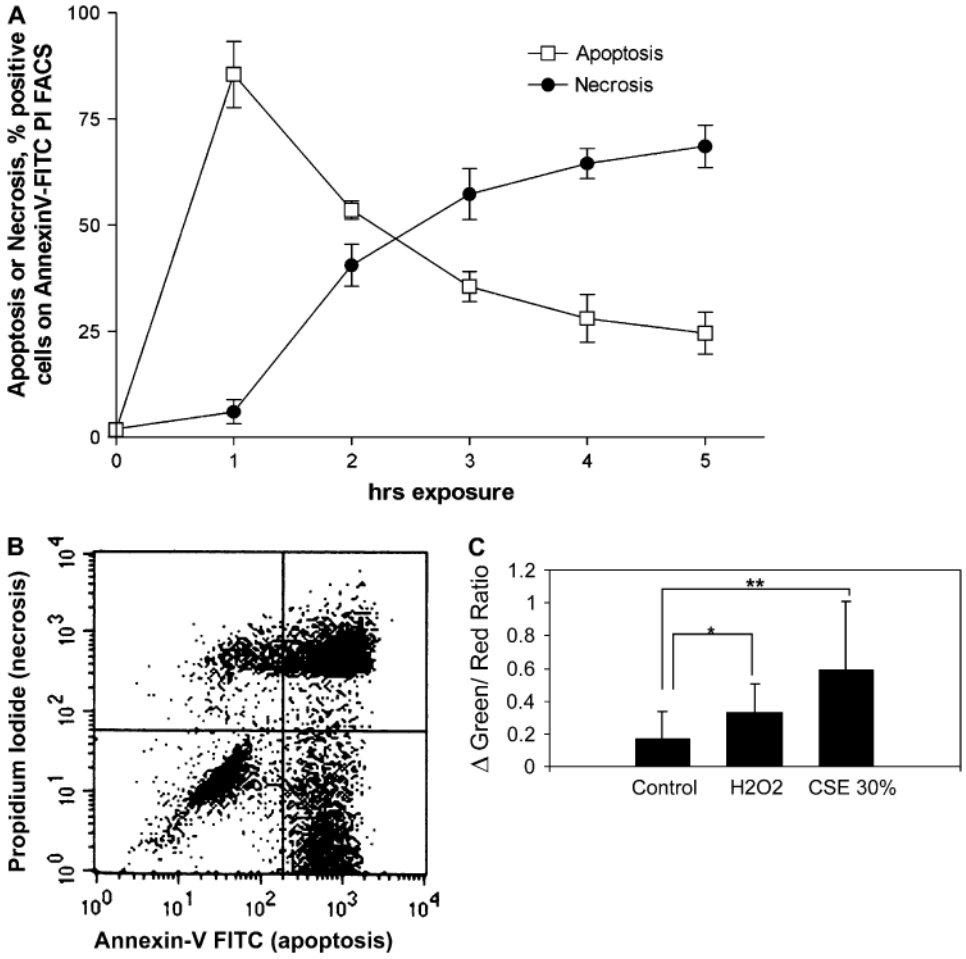

Figure 4. CSE induces apoptotic and necrotic cell death in Beas-2b cells. (*A*) Beas-2b cells were starved overnight in growth factor–free media, and then treated with 50% CSE for various time intervals (0–5 h). The percentage of cells positive for apoptosis or necrosis was determined by Annexin V–FITC/PI fluorescence-activated cell sorter analysis. Each data point represents the mean ± SD of three independent experiments. (*B*) A representative quadrant from cells exposed to 50% CSE for 3 h is displayed. (*C*) Normal Beas-2b at 50% confluence were loaded with JC-1 and then exposed to CSE (30%) or H_2O_2 (1 mM) as described in MATERIALS AND METHODS. The green:red fluorescence ratio, an indicator of mitochondrial depolarization, was taken at 30-s intervals at five different positions (20 cells each). Data represent the difference between the ratio at 20 min exposure and time of reagent addition, normalized to average baseline. Data are representative of the mean and SD, the average green:red ratio change of 20 cells at three to five positions per well. $^{**}P < 0.01$, $^{*}P < 0.05$.

umbilical vein endothelial cells, caspase-3 activation also mediated CSE-induced apoptosis (32–34). In contrast, Wickenden and colleagues recently reported that CSE-exposure caused strictly necrosis in A549 cells, with associated inhibition of apoptosis (35). In this model, the anti-apoptotic effects of CSE involved upstream inhibition of caspase-3/9 activation, and post-mitochondrial regulation of apoptosis-related factors to inhibit active apoptosome formation (35). Liu and coworkers also reported exclusively necrotic phenotypes in CSE-treated Beas-2b cells, with no activation of caspase-3 (36). In such studies, variations in experimental findings may occur in cell type–specific fashion, and may be further complicated by incomplete standardization of methodologies for experimental generation of CS, leading to variations in the strength of reported extract concentrations between individual laboratories. Additional limitations of CSE as a model of smoke exposure include the fact that some volatile compounds present in CS may be lost upon preparation of the extracts. Furthermore, the chemical composition of CSE may change upon handling or storage. Nevertheless recent consensus indicates that CSE remains a useful model of smoke exposure applicable to *in vitro* experiments with cultured cells (37).

In the current study we observe both apoptotic and necrotic cell death in Beas-2b cells exposed to CSE, with a transition from apoptosis to necrosis occurring with increasing duration (> 1 h) of CSE exposure (Figure 4A). This cellular death was associated with the early activation of caspase-3 (data not shown). CSE caused a depletion of cellular energy charge (ATP levels) in control cells (Figure 5A). Since mitochondria supply energy (ATP) for the apoptotic process, ATP levels may play a crucial role in the routing of cells to die by apoptosis or necrosis (11). Thus, depletion of cellular ATP by CSE may drive early apoptotic cells to switch to necrosis.

The inducible stress protein HO-1 confers protection against oxidative cellular injury and apoptosis in many disease models where ROS are implicated, including ischemia/reperfusion injury, hyperoxic stress/ acute lung injury, and atherosclerosis (19). Furthermore, adenoviral-mediated expression of HO-1 has also been shown to protect the mouse against experimental elastase–induced emphysema (38). We examined the potential relationship between HO-1 induction and CSE-related cell death. In attempting to characterize the general HO-1 induction response to CSE and other stress agents (hemin, LPS) in lung epithelial cells, we discovered a novel mitochondrial localization of HO-1 protein, and HO activity, which was strongest after CSE exposure. This response was observed in two types of transformed epithelial cell lines (Beas-2b, A549), as well as in a primary SAEC. Furthermore, this accumulation of HO-1 appeared dramatically more concentrated in mitochondria than in cytosol when normalized to the protein content of corresponding extracts (Figure 2C). Since its initial discovery in 1968, HO-1 has been described as a protein residing largely in the rough ER (15, 16). HO activity is abundant in microsomal ($104{,}000 \times g$) fractions containing cellular membranes, and can be isolated in association with NADPH: cytochrome p450 reductase and NAD(P)H: biliverdin reductase (39). HO-1 contains a carboxy terminal hydrophobic domain, which anchors this protein in cellular membranes (40, 41). Constitutive expression of the rat

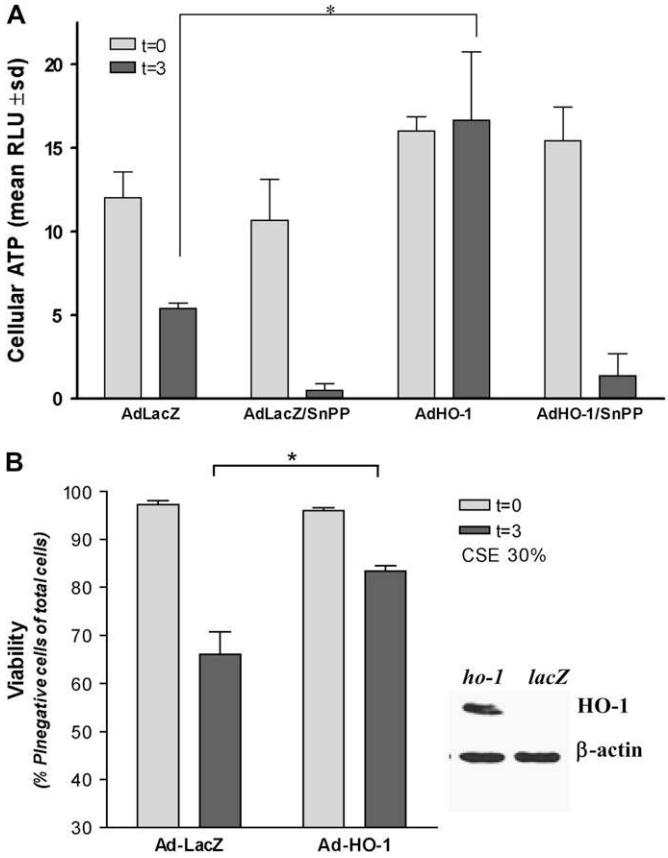

Figure 5. HO-1 protects against CSE-induced cell death and loss of ATP. Beas-2b cells were starved overnight in growth factor–free media, and then infected with Ad-HO-1 or Ad-LacZ for 6 h. At 24 h after transfection, cells were treated with 30% CSE for an additional 3 h, or sham treatment, in the absence or presence of SnPPIX (20 μM). After treatments, cells were analyzed for total ATP content (*A*), or assayed for cell viability by PI exclusion (*B*). Expression of HO-1 from the adenovirus was confirmed by Western immunoblot analysis (*B*, *insert*). β-Actin served as a standard for protein loading. $*P < 0.01$.

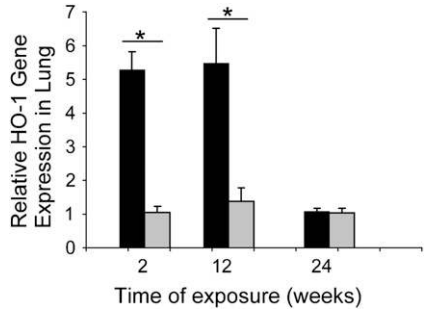

Figure 6. AKR/J mice were exposed to 24 wk of CS exposure (*black bars*) or air (*gray bars*) as described in MATERIALS AND METHODS. At 2, 12, and 24 wk exposure lungs were excised. Relative HO-1 gene expression in lung tissue was determined at each indicated exposure time, by real-time PCR as described in MATERIALS AND METHODS (n = 3–8 animals per time point per exposure condition). $*P < 0.01$.

HO-1 cDNA in animal cells indicated an ER localization of the expression product (40). Recent studies from our laboratories have shown the potential compartmentalization of HO-1 in other subcellular domains beside the ER, including the mitochondria and caveolae (23). Using sucrose density-gradient fractionation, we observed that hemin, hypoxia, and LPS stimulation alter the subcellular distribution pattern of HO-1 in lung endothelial cells, with accumulations in cytochrome c containing fractions, and detergent-resistant plasma membrane fractions (23).

Since the constitutive isozyme heme oxygenase-2 (HO-2) is refractory to most forms of chemical induction, including the agents under study, the observed induction of HO activity in mitochondrial fractions by CSE most likely represents the chemical induction of HO-1 by CSE constituents as confirmed by immunoblot analysis. However, since HO activity assays do not discriminate between HO-1 and HO-2 activity, the relative contribution of HO-2 to basal mitochondrial HO activity remains unclear. This issue may warrant the examination of the possible occurrence of HO-2 in mitochondria, as well as other enzymes that support heme-degradative activity, including NAD(P)H: biliverdin reductase (BVR), and NADPH: cytochrome p450 reductase (NPR). NPR was detected in the mitochondria of Beas-2b cells, consistent with a functional role for mitochondrial HO activity. BVR, while not essential for HO activity, provides the second step in the heme metabolic pathway. Its absence from the mitochondrial fraction is consistent with previous reports of primarily cytosolic or microsomal localization of this enzyme in various cell types (24). This observation also suggests that biliverdin is not likely metabolized in the mitochondria.

As previously hypothesized (42), the principal function of inducible HO-1 in the mitochondria may be to degrade accumulated heme. Mitochondria are critically involved in the heme biosynthetic pathway in that they contain the rate-limiting step (δ-aminolevulinic acid synthase) as well as the final enzymatic steps (coproporphyrinogen III oxidase, protoporphyrinogen IX oxidase, ferrochelatase) of this pathway. Newly synthesized hemes are used for the synthesis of various hemoproteins, including hemoglobin, myoglobin and cytochrome p450, and the mitochondrial cytochromes a-a_3, b, and c (43, 44). Free hemes (b, c) are known substrates for HO activity, but not in their protein-bound forms (43). In the mitochondria the source of heme as substrate for HO activity likely arises from the turnover of hemoprotein pools, which may accelerate under conditions of stress or mitochondrial dysfunction such as exposure to CSE. A recent study, which observed mitochondrial localization of HO-1 in rat liver, proposed that HO-1 serves a regulatory role by reducing the bioavailability of heme to support cytochrome-c: oxidase activity (45). In the context of neurological disorders, excessive induction of HO-1 has been associated with pathological mitochondrial iron deposition (46). In the current study, however, the overexpression of HO-1 in epithelial cells clearly preserved mitochondrial ATP production and prevented cell death, in the presence of CSE, implying anti-necrotic protection (Figure 5). Previously, HO-1 has been shown to inhibit cytokine-induced apoptosis in fibroblasts (47). Further studies are needed to elucidate the precise contributions of HO-derived end products such as CO, biliverdin, and/or iron to this metabolic protection. Among the byproducts of HO activity, the liberation of CO has been associated with antiapoptotic processes in endothelial cells, by activating p38β MAPK-dependent pathways (48). CO inhibits cellular respiratory chain activity *in vitro* at high concentration, and may increase mitochondrial ROS production at low concentration (49). The functional significance of small gas production, including nitric oxide and CO in the mitochondrial compartment, remain unclear though some have proposed a physiologic relevance for down-regulation of respiratory chain activity under conditions of cellular stress (50). The discovery that inducible HO-1 localizes in part to the mitochondria may be of broad

significance to the understanding of the mechanism(s) by which HO-1 confers protection against a wide variety of stimuli. An understanding of the function of the HO-1 enzyme system in the context of CSE-induced cellular and lung injury may provide potential therapeutic avenues, and increase the understanding of the etiology of smoke-related illness.

Conflict of Interest Statement: None of the authors has a financial relationship with a commercial entity that has an interest in the subject of this manuscript.

References

1. Pauwels RA, Rabe KF. Burden and clinical features of chronic obstructive pulmonary disease (COPD). *Lancet* 2004;364:613–620.
2. Barnes PJ, Shapiro SD, Pauwels RA. Chronic obstructive pulmonary disease: molecular and cellular mechanisms. *Eur Respir J* 2003;22:672–688.
3. Rahman I, MacNee W. Role of oxidants/antioxidants in smoking-induced lung diseases. *Free Radic Biol Med* 1996;21:669–681.
4. Rustemeier K, Stabbert R, Haussmann HJ, Roemer E, Carmines EL. Evaluation of the potential effects of ingredients added to cigarettes. Part 2: chemical composition of mainstream smoke. *Food Chem Toxicol* 2002;40:93–104.
5. Pauwels RA, Buist AS, Calverley PM, Jenkins CR, Hurd SS. GOLD Scientific Committee. Global strategy for the diagnosis, management, and prevention of chronic obstructive pulmonary disease. NHLBI/WHO Global Initiative for Chronic Obstructive Lung Disease (GOLD) Workshop summary. *Am J Respir Crit Care Med* 2001;163:1256–1276.
6. Shapiro SD, Ingenito EP. The pathogenesis of chronic obstructive pulmonary disease: advances in the past 100 years. *Am J Respir Cell Mol Biol* 2005;32:367–372.
7. Yokohori N, Aoshiba K, Nagai A. Respiratory Failure Research Group in Japan. Increased levels of cell death and proliferation in alveolar wall cells in patients with pulmonary emphysema. *Chest* 2004;125:626–632.
8. Imai K, Mercer BA, Schulman LL, Sonett JR, D'Armiento JM. Correlation of lung surface area to apoptosis and proliferation in human emphysema. *Eur Respir J* 2005;25:250–258.
9. Hageman GJ, Larik I, Pennings HJ, Haenen GR, Wouters EF, Bast A. Systemic poly (ADP-ribose) polymerase-1 activation, chronic inflammation, and oxidative stress in COPD patients. *Free Radic Biol Med* 2003;35:140–148.
10. Green DR, Reed JC. Mitochondria and apoptosis. *Science* 1998;281:1309–1312.
11. Leist M, Single B, Castoldi AF, Kuhnle S, Nicotera P. Intracellular adenosine triphosphate (ATP) concentration: a switch in the decision between apoptosis and necrosis. *J Exp Med* 1997;185:1481–1486.
12. Gairola C, Aleem MI. Cigarette smoke: effect of aqueous and nonaqueous fractions on mitochondrial function. *Nature* 1973;241:287–288.
13. Smith PR, Cooper JM, Govan GG, Harding AE, Schapira AH. Smoking and mitochondrial function: a model for environmental toxins. *Q J Med* 1993;86:657–660.
14. Miro O, Alonso JR, Jarreta D, Casademont J, Urbano-Marquez A, Cardellach F. Smoking disturbs mitochondrial respiratory chain function and enhances lipid peroxidation on human circulating lymphocytes. *Carcinogenesis* 1999;20:1331–1336.
15. Tenhunen R, Marver HS, Schmid R. Microsomal heme oxygenase, characterization of the enzyme. *J Biol Chem* 1969;244:6388–6394.
16. Tenhunen R, Marver HS, Schmid R. The enzymatic conversion of heme to bilirubin by microsomal heme oxygenase. *Proc Natl Acad Sci USA* 1968;61:748–755.
17. Morse D, Choi AM. Heme oxygenase-1: from bench to bedside. *Am J Respir Crit Care Med* 2005;172:660–670.
18. Slebos DJ, Ryter SW, Choi AM. Heme oxygenase-1 and carbon monoxide in pulmonary medicine. *Respir Res* 2003;4:7.
19. Ryter S, Otterbein LE, Morse D, Choi AM. Heme oxygenase/ carbon monoxide signaling pathways: regulation and functional significance. *Mol Cell Biochem* 2002;234/235:249–263.
20. Slebos DJ, Kerstjens HA, Rutgers SR, Kauffman HF, Choi AM, Postma DS. Heme oxygenase-1 expression is diminished in alveolar macrophages of patients with COPD. *Eur Respir J* 2004;23:652–653.
21. Yamada N, Yamaya M, Okinaga S, Nakayama K, Sekizawa K, Shibahara S, Sasaki H. Microsatellite polymorphism in the heme oxygenase-1 gene promoter is associated with susceptibility to emphysema. *Am J Hum Genet* 2000;66:187–195.
22. Lomas DA, Silverman EK. The genetics of chronic obstructive pulmonary disease. *Respir Res* 2001;2:20–26.
23. Kim HP, Wang X, Galbiati F, Ryter SW, Choi AM. Caveolae compartmentalization of heme oxygenase-1 in endothelial cells. *FASEB J* 2004;18:1080–1089.
24. Ryter SW, Kvam E, Tyrrell RM. Heme oxygenase activity: current methods and applications. *Methods Mol Biol* 2000;99:369–391.
25. Witschi H, Espiritu I, Maronpot RR, Pinkerton KE, Jones AD. The carcinogenic potential of the gas phase of environmental tobacco smoke. *Carcinogenesis* 1997;18:2035–2042.
26. Rangasamy T, Cho CY, Thimmulappa RK, Zhen L, Srisuma SS, Kensler TW, Yamamoto M, Petrache I, Tuder RM, Biswal S. Genetic ablation of Nrf2 enhances susceptibility to cigarette smoke-induced emphysema in mice. *J Clin Invest* 2004;114:1248–1259.
27. Hoshino Y, Mio T, Nagai S, Miki H, Ito I, Izumi T. Cytotoxic effects of cigarette smoke extract on an alveolar type II cell-derived cell line. *Am J Physiol Lung Cell Mol Physiol* 2001;281:L509–L516.
28. Vayssier M, Banzet N, Francois D, Bellmann K, Polla BS. Tobacco smoke induces both apoptosis and necrosis in mammalian cells: differential effects of HSP70. *Am J Physiol* 1998;275:L771–L779.
29. Aoshiba K, Tamaoki J, Nagai A. Acute cigarette smoke exposure induces apoptosis of alveolar macrophages. *Am J Physiol Lung Cell Mol Physiol* 2001;281:L1392–L1401.
30. Carnevali S, Petruzzelli S, Longoni B, Vanacore R, Barale R, Cipollini M, Scatena F, Paggiaro P, Celi A, Giuntini C. Cigarette smoke extract induces oxidative stress and apoptosis in human lung fibroblasts. *Am J Physiol Lung Cell Mol Physiol* 2003;284:L955–L963.
31. D'Agostini F, Balansky RM, Izzotti A, Lubet RA, Kelloff GJ, De Flora S. Modulation of apoptosis by cigarette smoke and cancer chemopreventive agents in the respiratory tract of rats. *Carcinogenesis* 2001;22:375–380.
32. Wang H, Ma L, Li Y, Cho CH. Exposure to cigarette smoke increases apoptosis in the rat gastric mucosa through a reactive oxygen species-mediated and p53-independent pathway. *Free Radic Biol Med* 2000;28:1125–1131.
33. Wang HY, Shin VY, Leung SY, Yuen ST, Cho CH. Involvement of bcl-2 and caspase-3 in apoptosis induced by cigarette smoke extract in the gastric epithelial cell. *Toxicol Pathol* 2003;31:220–226.
34. Wang J, Wilcken DE, Wang XL. Cigarette smoke activates caspase-3 to induce apoptosis of human umbilical venous endothelial cells. *Mol Genet Metab* 2001;72:82–88.
35. Wickenden JA, Clarke MC, Rossi AG, Rahman I, Faux SP, Donaldson K, MacNee W. Cigarette smoke prevents apoptosis through inhibition of caspase activation and induces necrosis. *Am J Respir Cell Mol Biol* 2003;29:562–570.
36. Liu X, Conner H, Kobayashi T, Kim H, Wen F, Abe S, Fang Q, Wang X, Hashimoto M, Bitterman P, *et al.* Cigarette smoke extract induces DNA damage but not apoptosis in human bronchial epithelial cells. *Am J Respir Cell Mol Biol* 2005;33:121–129.
37. Rennard SI. Cigarette smoke in research. *Am J Respir Cell Mol Biol* 2004;31:479–480.
38. Shinohara T, Kaneko T, Nagashima Y, Ueda A, Tagawa A, Ishigatsubo Y. Adenovirus-mediated transfer and overexpression of heme oxygenase 1 cDNA in lungs attenuates elastase-induced pulmonary emphysema in mice. *Hum Gene Ther* 2005;16:318–327.
39. Yoshinaga T, Sassa S, Kappas A. The occurrence of molecular interactions among NADPH-cytochrome c reductase, heme oxygenase, and biliverdin reductase in heme degradation. *J Biol Chem* 1982;257:7786–7793.
40. Shibahara S, Muller RM, Taguchi H, Yoshida T. Cloning and expression of cDNA for rat heme oxygenase. *Proc Natl Acad Sci USA* 1985;82:7865–7869.
41. Yoshida T, Biro P, Cohen T, Müller M, Shibahara S. Human heme oxygenase cDNA and induction of its mRNA by hemin. *Eur J Biochem* 1988;171:457–461.
42. Keyse SM, Tyrrell RM. Heme oxygenase is the major 32-kDa stress protein induced in human skin fibroblasts by UVA radiation, hydrogen peroxide, and sodium arsenite. *Proc Natl Acad Sci USA* 1989;86:99–103.
43. Maines MD. Heme oxygenase: function, multiplicity, regulatory mechanisms, and clinical applications. *FASEB J* 1988;2:2557–2568.
44. Ryter S, Tyrrell RM. The heme synthesis and degradation pathways, role in oxidant sensitivity. Heme oxygenase has both pro- and anti-oxidant properties. *Free Radic Biol Med* 2000;28:289–309.
45. Converso DP, Taille C, Carreras MC, Jaitovich A, Poderoso JJ, Boczkowski J. HO-1 is located in liver mitochondria and modulates mitochondrial heme content and metabolism. *FASEB J* 2006;20:1236–1238.

46. Mehindate K, Sahlas DJ, Frankel D, Mawal Y, Liberman A, Corcos J, Dion S, Schipper HM. Proinflammatory cytokines promote glial heme oxygenase-1 expression and mitochondrial iron deposition: implications for multiple sclerosis. *J Neurochem* 2001;77:1386–1395.
47. Petrache I, Otterbein LE, Alam J, Wiegand GW, Choi AM. Heme oxygenase-1 inhibits TNF-alpha-induced apoptosis in cultured fibroblasts. *Am J Physiol Lung Cell Mol Physiol* 2000;278:L312–L319.
48. Brouard S, Otterbein LE, Anrather J, Tobiasch E, Bach FH, Choi AM, Soares MP. Carbon monoxide generated by heme oxygenase-1 suppresses endothelial cell apoptosis. *J Exp Med* 2000;192:1015–1026.
49. Taille C, El-Benna J, Lanone S, Boczkowski J, Motterlini R. Mitochondrial respiratory chain and NAD(P)H oxidase are targets for the antiproliferative effect of carbon monoxide in human airway smooth muscle. *J Biol Chem* 2005;27:25350–25360.
50. Moncada S, Erusalimsky JD. Does nitric oxide modulate mitochondrial energy generation and apoptosis? *Nat Rev Mol Cell Biol* 2002;3:214–220.